

The building-up of phase diagrams*

Jorge C. G. Calado and José N. Canongia Lopes

Centro de Química Estrutural, Instituto Superior Técnico, 1049-001 Lisboa, Portugal

Abstract: This paper begins with a bird's-eye view of the history of phase equilibrium diagrams for mixtures, their classification and interpretation. Running throughout the discussion are the fertile ideas of van der Waals. The Scott and van Konynenburg classification is revisited, and various types of phase diagrams are generated by computer simulation, using the Gibbs Ensemble Monte Carlo Method for one-centre 12-6 Lennard-Jones molecules. The work is hopefully made more attractive and appealing to students by a judicious choice of architectural and engineering equivalents.

INTRODUCTION

It is a truth universally acknowledged, that the purpose of science is to bring order upon the world. The *Encyclopaedia Britannica* defines science as 'a mood in which the world is considered' [1]. It is a mood that enables the observer to make sense of that same world. Like any creator, the scientist begins his or her task by naming the new and classifying what is already known. Devising a workable nomenclature and terminology system is the first duty of a pioneer in any field. With names (nouns) and ideas a memory palace can be built; the learning process can then follow. The eighteenth century—the age of the Enlightenment—gave us the classification of all things created: minerals and rocks, plants and animals. We owe to Carl von Linné (1707–1778) the principles for defining genera and species, and the generalised use of the binomial system for naming plants [2] and animals. Later, the classification mania spread even to shapeless and ever-changing things like clouds. In 1803 Luke Howard (1772–1864) separated the clouds and gave them names—the names for which they are known today: cumulus, cirrus, stratus, etc.—and founded the new science of meteorology. Howard's essay 'On the Modifications of Clouds...' [3] had a far-reaching influence on the arts (poetry, painting) of his time.

As the diversity increases, problems multiply. Chemistry deals with more than a million molecules, but with only about one hundred useful atoms. In fact, most of us go through (scientific) life using no more than a couple of dozen different atoms or, in many cases, a mere half a score. Even so, the structural possibilities are countless (one has only to think of the carbon and silicon atoms and the variety of molecular structures that they generate). Fortunately, nature imitates itself. The same patterns and structures seem to recur everywhere. The logarithmic spiral (or a good approximation of it)—to take but one example—appears as the basis of the Nautilus shell or of the arrangement of seeds in the sunflower. For the thermodynamicist interested in the properties of mixtures and solutions, the big challenge is the understanding of how they react to changes of temperature, pressure, composition, etc.—in other words, the classification and prediction of the phase diagrams.

ENTER VAN DER WAALS

Order came late to phase equilibria. There was the lonely visionary, Josiah Willard Gibbs (1839–1903) with his Phase Rule and free energy, and then there was Johannes Diderik van der Waals (1837–1923)

*Lecture presented at the 15th International Conference on Chemical Thermodynamics, Porto, Portugal, 26 July–1 August 1998, pp. 1167–1306.

with his equation of state,

$$(p + a/V^2)(V - b) = RT \quad (1)$$

p , V and T are, as usual, the pressure, molar volume and temperature; R is the gas constant and a and b are parameters related to the cohesive energy and molecular size, respectively. Like many other developments in the thermodynamics of fluids, we owe the first understanding of the phase behaviour of binary mixtures to van der Waals. In 1889, 16 years after the defence of his academic thesis ‘Over de Continuïteit van den Gas- en Vloeistoftoestand’ (On the Continuity of the Gaseous and Liquid States) [4], van der Waals presented, at a meeting of the Academy of Sciences in Amsterdam, a concise report on a molecular theory of a mixture of two components, later published in an extended form as ‘Théorie moléculaire d’une substance composée de deux matières différentes’ (A molecular theory of a substance composed of two different species) [5]. In this paper van der Waals generalised his equation of state to binary mixtures of mole fraction x , and proposed a quadratic expression on the composition for the calculation of the mixture parameter $a(x)$. To some extent, he was following the steps of Hendrik Antoon Lorentz (1853–1928) who had shown that, for a binary mixture, the co-volume $b(x)$ should be given by a similar quadratic expression [6].

Van der Waals had obviously been inspired by the theoretical work of Gibbs. (Along with James Clerk Maxwell (1831–1879), Gibbs remained, throughout the Dutch physicist’s life, one of his scientific idols.) Already in 1888–89, van der Waals had given, at the University of Amsterdam, a course of lectures on the molecular theory of mixtures. More or less at the same time, his younger colleague at Leiden, Heike Kamerlingh Onnes (1853–1926), was planning a systematic and ambitious program to study the experimental behaviour of mixtures. Once again, experiment would follow theory. (As a matter of fact, van der Waals would eventually dedicate the second part of his theory of mixtures to Onnes [7].)

Basically, what van der Waals did was to apply a corresponding states treatment to mixtures under the so-called one-fluid approximation (‘Naturally all questions that were unanswered for a single substance remain unanswered for the mixture’, he wrote in the *2er Teil* of his magnum opus [7]). Van der Waals established the rules for the coexistence of different phases, touched upon azeotropy and liquid-liquid immiscibility and discussed the effect of the values of the ratio $a(x)/b(x)$ relative to those for the pure components. Moreover, he considered the added complication of association (dimerization of one component) and the influence of an external field such as gravity; mechanical instability and spinodal curves were also dealt with. Meanwhile in Leiden, Kamerlingh Onnes and his collaborators (J. P. Kuenen among them) proceeded with their experimental investigation of mixtures under wide ranges of temperature and pressure. It was Kuenen who found and understood, in the carbon dioxide + methyl chloride system [8], the phenomenon of ‘retrograde condensation’ (the increase, in a liquid-vapour situation, of the amount of liquid by a reduction of pressure).

Soon this type of research spread to other countries, namely Belgium, England, Germany. The world seemed ready for a proper classification and interpretation of the various types of phase diagrams. All the facts were in place, even the right handles: lots of good experimental data, a remarkably insightful equation of state, and the recognition of the importance, in any discussion, of the relative values of the parameter ratios. However, despite its apparent simplicity, van der Waals’ equation of state for mixtures proved—at the time—too complicated for its capabilities to be fully tested by its creator, his contemporaries or immediate followers. It had too many variables and parameters—pressure, temperature, composition, a trio of aa and a trio of bb . The use of ratios (a_{22}/a_{11} , a_{12}/a_{11} , etc.) and the assumption that the molecules had the same size (identical values of b) simplified the problem somehow, but not enough. Van der Waals’s last paper, still on the theory of binary mixtures, appeared in 1913 [9]. He was 76 years old. Soon, the Great War made experimental research difficult. The enthusiasm for the theoretical treatment of mixtures petered out after World War I.

There were other reasons for the decline. The emphasis had moved, in the Dutch school, from high pressure to low temperature studies. In 1911, Kamerlingh Onnes discovered the phenomenon of superconductivity in mercury, at temperatures close to the absolute zero [10]. The world of physics was witnessing its biggest revolution since the days of Newton. A new paradigm, founded on a space-time continuum and the marvels of atomic theory, was advancing. The great rage was relativity and quantum mechanics; fluids and their mixtures were no longer fashionable or deemed interesting. To become

beautiful again, thermodynamics had to wait for the development of a quantum theory of intermolecular forces.

THE TURN OF THE SUPERPOWERS

If the theoretical understanding of fluid mixtures had to be put on a back burner, experiments were proceeding apace, mainly in connection with the gas and oil industries. In the 1930s resourceful chemical engineers in America embarked on systematic experimental programs to map out the phase diagrams of hydrocarbon mixtures up to their critical lines. The most productive groups were those at MIT, Ohio State and CalTech led by L. W. T. Cummings, W. B. Kay and B. H. Sage and W. N. Lacey, respectively [11]. The technological and economic importance of natural gas, petrochemical products and their derivatives, and of supercritical extraction in the food industry has kept phase diagrams at the forefront of chemical engineering up to the present day. After World War II, Russian work carried out by Krichevskii and Tsiklis up and beyond pressures of one kilobar became available [12]. To this list, and without being exhaustive, the name of R. Kobayashi (who did beautiful research in high-pressure thermodynamics at Rice University) should be added. In Germany, E. U. Franck in Karlsruhe, G. M. Schneider in Bochum and H. Knapp in Berlin also made major contributions in this area [13] in the 1970s and 1980s, as has J. de Swaan Arons in Delft. A particular case that deserves attention is that provided by the atmospheres of the outer planets and their satellites. These are giant laboratories operating under extreme conditions of temperature and/or pressure. Inevitably, the age of space exploration inspired thermodynamicists to look into systems relevant to planetary bodies. W. B. Streett and collaborators, first at the Science Research Laboratory at West Point and then at Cornell University, investigated a whole series of binary systems containing hydrogen and/or helium—the major components of the giant planets [14].

Meanwhile, the problems posed by fluid mixtures had become more interesting and appealing to physical chemists and theoreticians. Joseph O. Hirschfelder, at the Naval Research Laboratory of the University of Wisconsin, began applying the methods of statistical mechanics and quantum mechanics to the studies of fluids, a work which culminated in the publication in 1954 of his masterpiece (in collaboration with C. F. Curtiss and R. Byron Bird), *Molecular Theory of Gases and Liquids* [15]. From then on, the understanding and classification of phase diagrams has been irrevocably linked to the knowledge of intermolecular forces.

THE MOLECULAR POINT OF VIEW

In science, it is often the simplest models that yield the deepest insights. This is what happens in molecular thermodynamics. For instance, computer simulations have shown that, as the density increases, the structure of an assembly of hard spheres (billiard balls) can dramatically change from a disordered state to a closed-packed crystal lattice [16]. In other words, the phenomenon of melting (or solidification)—the first-order transition between an ordered and a disordered state—is a consequence of repulsive forces alone. No assumption about attractive forces is needed for the phenomenon to occur. These findings were seen as one of the most exciting and beautiful discoveries of the early 1960s in the field of thermodynamics.

Experience has also shown that it is not necessary to invoke sophisticated theories to understand the diversity of phase diagrams, even at high pressures. Relatively primitive models and equations have proved versatile enough to generate most types of phase behaviour known to experimentalists. A case in point is that posed by the 12–6 Lennard-Jones potential, $u(r)$,

$$u(r) = 4\epsilon[(r/\sigma)^{12} - (r/\sigma)^6] \quad (2)$$

where ϵ and σ are the intermolecular parameters and r is the distance between molecules. An effective high-density potential at best (it is softer and shallower than the true pair potential), the Lennard-Jones function can nevertheless be extremely useful in computer simulation and the testing of statistical theories. Another very prolific tool is the van der Waals equation of state itself. Intermolecular potentials and equations of state work in tandem, the former being the microscopic counterpart of the latter. It should be noted that van der Waals's equation is equivalent to a hard-sphere potential onto which a

weekly attractive potential of very long range has been superimposed. In the limit, the depth of the potential is infinitesimal and its range is infinite.

It was only in the early 1970s, with the development of faster computers, that the potentialities of the van der Waals equation could be fully appreciated. The seminal contribution here is that of Scott and van Konynenburg, which appeared in an extended version under the title 'Critical lines and phase equilibria in binary van der Waals mixtures' [17]. It is a tribute to the insight and prescience of its authors (and to the genius of van der Waals) that their classification has remained almost unchanged for over 20 years. Scott and van Konynenburg showed that the application of the van der Waals equation of state to mixtures predicted, in a qualitative way, almost all types of phase equilibria that had been found experimentally, and indeed they were even able to postulate the existence of a few other subtypes which had not been discovered in the laboratory. In their paper, Scott and van Konynenburg defined altogether six types of phase diagrams, which they grouped into three main classes. These can be best understood considering their (p , T) projections (Fig. 1).

Types I and II form Class 1, i.e. mixtures of two components with similar gas-liquid critical temperatures where the critical points of the two pure components are connected by a continuous critical line. Class 2 includes types III to V where the critical line is not continuous, either because it diverges from the critical point of the less volatile component to a high-pressure compact state, or because of the intromission of the three-phase line. Class 3 corresponds to type VI where phenomena such as the occurrence, in the low-temperature region, of a lower critical solution temperature along with that of an upper critical solution temperature, lead to the formation of a closed-loop immiscibility window. In general, the classification into classes is omitted in the literature.

Some of the types can be further subdivided into two or more subtypes referring to secondary features of the corresponding phase diagrams. As an example, type I can be divided into type I-proper and type IA, where A stands for azeotrope. Other studies, using different equations of state, have predicted new types and subtypes of phase diagrams [18,19]. For instance, Boshkov and Mazur [18] foresaw the occurrence of a type VII diagram for Lennard-Jones mixtures. (Type VII is similar to type V, but exhibits closed-loop immiscibility behaviour at low temperatures.) As new types and subtypes have been added to the original list (more than 20 varieties have been reported), the need for a new classification became urgent. Recently, Bolz, Deiters, Peters and de Loos proposed a new system of classification based on the number of critical lines and their end-points [20].

THE OVERALL PICTURE

A global phase diagram is a chart connecting the molecular and macroscopic worlds: the former is defined by reduced variables which are ratios of molecular parameters; the latter refers to the various types of phase diagrams found in the laboratory. In other words, the coordinates of the chart (longitude, latitude) belong to the microscopic world, but the domains defined by the lines on the map (countries) correspond to the macroscopic behaviour of different types of mixtures (Fig. 2).

If a binary mixture is modeled by a bi-parametric equation of state or intermolecular potential, four parameters are needed to characterize the global phase diagram. These correspond to the four independent energy and size ratios for the hetero and homo interactions. For the sake of simplicity, they are usually reduced to two assuming, for instance, that the molecules have the same size and that they follow the Lorentz combining rule (arithmetic mean of diameters). In the case of the van der Waals equation, the chosen parameters are often ζ and λ , defined as [17]:

$$\zeta = (a_{22} - a_{11})/(a_{11} + a_{22}) \quad (3)$$

$$\lambda = (a_{11} - 2a_{12} + a_{22})/(a_{11} + a_{22}) \quad (4)$$

As for the Lennard-Jones intermolecular potential, the four parameters are Z_1 to Z_4 , defined as

$$Z_1 = (\epsilon_{22} - \epsilon_{11})/(\epsilon_{22} + \epsilon_{11}) \quad (5)$$

$$Z_2 = (\epsilon_{22} - 2\epsilon_{12} + \epsilon_{11})/(\epsilon_{22} + \epsilon_{11}) \quad (6)$$

$$Z_3 = (\sigma_{22} - \sigma_{11})/(\sigma_{22} + \sigma_{11}) \quad (7)$$

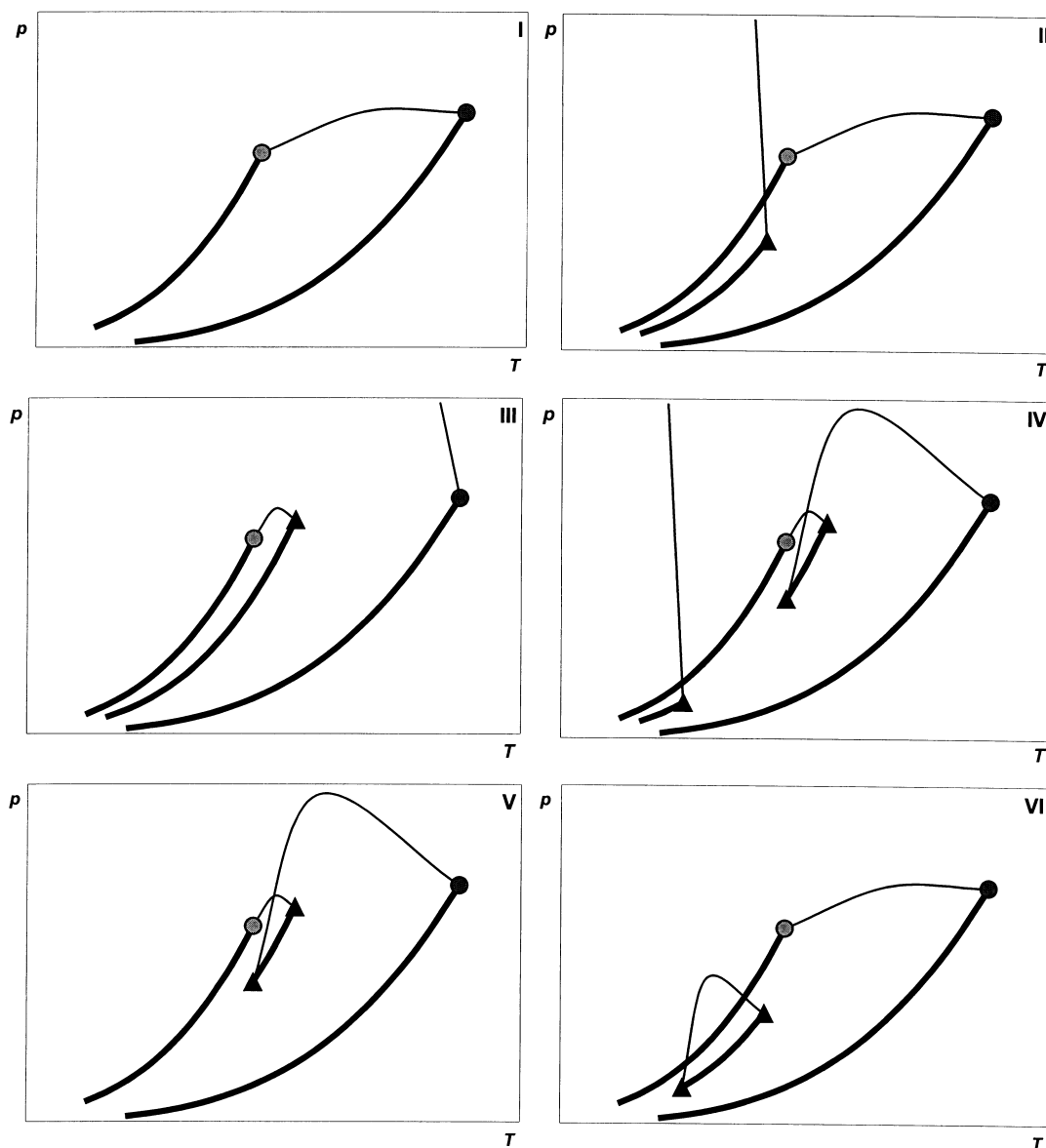


Fig. 1 Fluid phase diagrams (p - T projections) representing six types (I to VI) of binary mixtures (adapted from [17]). The thick lines represent either the saturation curves of the two pure components or three-phase lines of their mixtures. The latter end at the critical points of each pure substance (circles) or at the upper/lower critical end points (triangles) of the mixtures. The thin lines represent the loci of the liquid-liquid or gas-liquid mixture critical points (critical lines of the mixtures).

$$Z_4 = (\sigma_{22} - 2\sigma_{12} + \sigma_{11})/(\sigma_{22} + \sigma_{11}) \quad (8)$$

(These can, of course, be reduced to two, Z_1 and Z_2 , if assumptions similar to those defined above for the van der Waals equation are applied, cf. Fig. 2). As a rule-of-thumb, ζ or Z_1 reflect volatility differences between the two components, whereas λ or Z_2 indicate the relative weakness/strength of the crossinteraction energy parameter; Z_3 measures the molecular size difference and Z_4 the 'excess volume' (the relative weakness/strength of the cross-diameter parameter).

STRUCTURE AND ARCHITECTURE

The idea that the great diversity of phase behaviour found in nature can be harnessed by a logic classification system is a leap of the imagination as impressive as that that led Luke Howard to modify

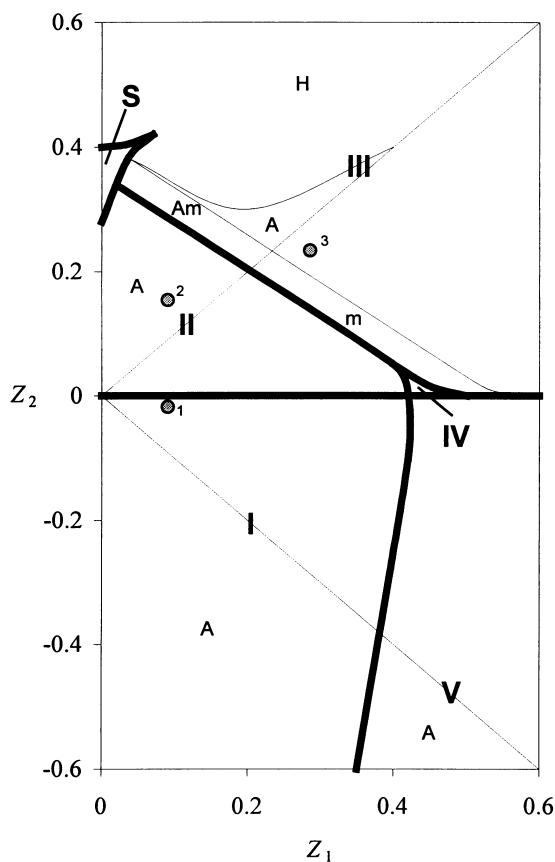


Fig. 2 Global phase diagrams for binary mixtures interacting via the one-centre Lennard-Jones (12-6) potential (adapted from [18]). The diagram shows the existence of a given mixture type (roman numeral) as a function of molecular parameters ratios (see text for the definition of Z_1 and Z_2). Types VI and VII (not shown) are also present in small regions around the area corresponding to type IV behaviour. Thick lines define the boundaries between different types of mixture; thin lines divide these domains into several subtypes (letters); the area marked as 'S' is the so-called shield region. The three points marked in arabic numerals show the location of the first three mixtures studied by computer simulation in this work.

and classify (and then baptise) clouds. Clouds, however, can be seen (and thus apprehended) by everyone with the naked eye. Students of thermodynamics can, at best, gather phase equilibria data in the laboratory. The way all these experimental points are brought together into lines, surfaces and volumes—the building-up of phase diagrams—often escapes them. In the age of the image (photography, television, video, advertising, etc.) people can no longer visualise in abstract, especially in three dimensions.

To fully comprehend the workings of a phase diagram, one has to inhabit a multidimensional space (hyperspace) where the variables are pressure, temperature, volume or density, composition, sometimes the chemical potential (or, even better, the activity). In the classroom, teachers use videos and draw projections and cross-sections on the blackboard and hope (against hope) that the students will make the leap to the overall picture. After all, anyone with a modicum of culture can visualise how the three-dimensional house will look, just from examining the two-dimensional sketches on the architect's drawing-board! A four-dimensional structure can, likewise, be conceived from its projections (volumes) on to three-dimensional space. However, in over 30 years of teaching experience, one of us (J.C.G.C.) has found again and again that, with the exception of the best and brightest, the majority of thermodynamics students has serious difficulties in grasping the whole picture—the implications of a phase equilibria diagram. To see is to believe. For the modern citizen, what cannot be seen (on TV, preferably) does not exist.

This frustration has led us to devise a novel approach to the teaching of phase diagrams. The starting point is the belief that nature is the great architect, and that men and women, in their constructs, merely follow and copy the workings of nature. It is a belief that goes back to, at least, the times of Leonardo da Vinci (1452–1519), whose prodigious inventions derived, to a large extent, from his observations of nature. Examples abound: the flying machine with its bird-like aviator flapping the wings through foot pedals, or the way da Vinci exploited engineering principles similar to those used in the human body to sustain the weight of the head. The mechanics of the skeleton and the elastic tensions of the muscle and tendon systems were always on his mind when busy devising useful engineering tools and contraptions.

The laws of science are the laws of nature and these cannot be violated. Progress follows the discovery (or invention) of new materials, with unique properties. In what concerns structures, engineers and architects often reproduce, consciously or unconsciously, what nature had already fabricated (sometimes at the molecular level). Conversely, if the engineer or the architect has found yet another simple economic solution to a structural problem (a useful criterion of beauty), then it usually follows that the chemist can translate it at the microscopic level by synthesising a new molecule. Take, as an example, the Bank of China in Hong Kong (1982–89), designed by I. M. Pei (Fig. 3). With its multifaceted elegance, it towers above the equally famous Hong Kong and Shanghai Bank, built by Norman Foster in 1981–86. Inevitably, sooner or later someone would synthesise a molecule of similar shape. It happened in 1994 when Hartl and Mahdjour-Hassan-Abadi [21] published the structure of the first compound (an iodocuprate) with a helical chain of face-sharing tetrahedra (Fig. 3). It is also no coincidence that Buckminster Fuller (1895–1983), as an engineer, had got there first, calling the structure a ‘tetrahelix’.

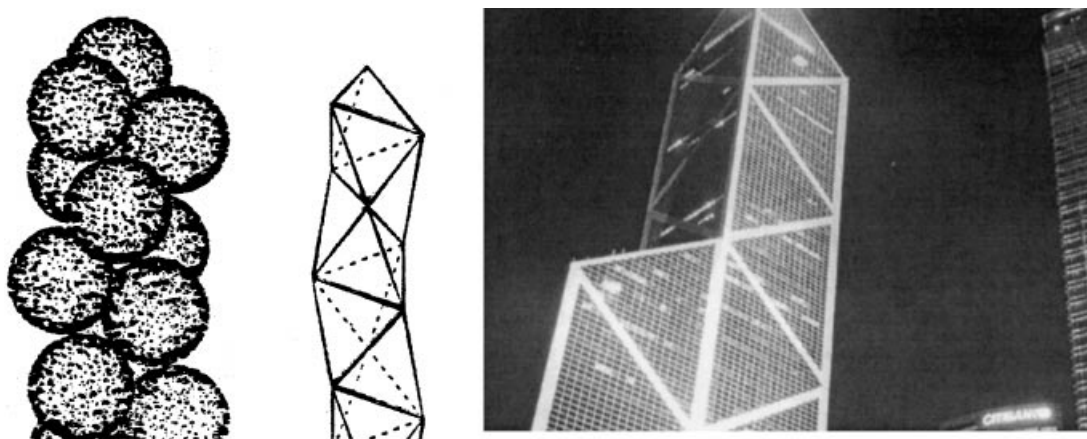


Fig. 3 The tetrahelix structures of the iodocuprate compound $[(C_6H_5)P]_{\infty}[Cu_3I_4]$ ([21], 1994) and of the Bank of China designed by I. M. Pei (Hong Kong, China, 1982–89).

It is cross-references, parallels and feedbacks like these that led us to accompany the description of the various types of phase diagrams that follow (generated by Monte Carlo simulation), by a world tour of architectural sites. This odd coupling should be seen as a tentative pædagogical aid to the visualisation and understanding of complex phase equilibria.

PHASE DIAGRAM SIMULATION

Global phase diagrams for a given molecular model can be built through the topological analysis of the corresponding equation of state. In the case of an analytical equation of state, like that of van der Waals, the model and the equation coincide; in the case of a fluid defined by an interaction potential, the corresponding equation of state, with a few exceptions (hard spheres, etc.), is no longer analytical and has to be obtained through computer simulation or any other suitable tool within the framework of statistical mechanics.

The problem is the following: the building-up of phase diagrams is based on the analysis of an equation of state, not of the intermolecular potential itself. Empirical or semi-empirical equations of state, like the one proposed by van der Waals, are usually of limited practical use: they apply only to a few systems or families of systems, under narrow conditions of pressure and temperature. On the other hand, realistic intermolecular potentials do not lend themselves to a feasible analytical treatment. It should be added that, from a strictly experimental point of view, studies limited to a few systems do not require the knowledge of the entire global phase diagram; conversely, the existing global phase diagrams are limited to a few molecular size ratios or to a specific type of potential and, as such, do not describe a wide variety of real systems. It is within this context that it can be said that molecular computer simulation fills the gap between theory and experiment.

It may sound a contradiction, but from the theoretical point of view, simulation studies can be used as 'experimental data'. Simulations with molecules modeled by the intermolecular potential underlying a particular equation of state can probe different types of phase behaviour and test the validity of the approximations performed in the construction of the corresponding global phase diagram.

Direct simulation of multiphase equilibria can also be used to interpret experimental data and even to predict phase behaviour once the modeling of a given system is well established. The advantages are clear: intermolecular potential parameters can be easily changed to fit experimental data, potentials can be chosen to describe the molecules in the most adequate way (they do not need to be the same for both components) and no knowledge about the equation of state is required. However, it should be remembered that this *modus operandi* represents a trade-off: the substitution of a more flexible, albeit less systematic, scheme (direct phase diagram simulation) for an intensive strategy (equation of state analysis). New territories can be mapped out simultaneously by the meticulous cartographer and the versatile explorer. Their actions and methods are complementary.

Several simulation techniques are on offer, but the Gibbs Ensemble Monte Carlo (GEMC) Method has proved to be one of the most effective ways of simulating two coexisting phases in equilibrium [22]. In the GEMC method, the coexisting phases are simulated in two separate subsystems (simulation boxes) that constitute the so-called Gibbs Ensemble. This avoids the direct simulation of the interface between the two bulk phases. Equilibrium is reached by allowing three types of Monte Carlo moves within and between the simulation boxes: particle displacements inside each subsystem, volume exchange between boxes (with the total volume kept constant) and particle transfer from one box to another (with the total number of particles and composition kept constant). While the first type of move is responsible for the internal equilibrium of each subsystem, the last two ensure that both the pressure and chemical potential of each component reach equality between subsystems (Fig. 4).

Recently, this method was extended to the study of more than two phases in equilibrium [23], allowing the simulation to occur in a number of simulation boxes matching the number of coexisting phases. The extension is particularly relevant to the present case since five out of the six types of phase diagram proposed by Scott and van Konynenburg exhibit three-phase lines (Fig. 1). In the following subsection, computer simulations of phase equilibria corresponding to several types of phase diagrams are described and the results discussed.

SIMULATION RESULTS

The five phase diagrams presented in this section (Fig. 5) were built using p - T - x data obtained by simulation using particles interacting via the one-centre Lennard-Jones [6,12] potential, within the framework of the constant volume GEMC method [24]. Each simulation run was performed using a system comprising 500 to 900 particles at fixed temperature and global density and composition. The number of phases present in each case is not defined *a priori*: if a sufficiently large number of simulation boxes is used, the simulation will evolve spontaneously until the correct number of phases, their composition and density and the equilibrium pressure are reached. The lines representing the complete phase boundaries shown in Fig. 5 are drawn only as visual guides.

Each individual diagram illustrates a different type of binary mixture whose characteristics (in terms of molecular parameters) are given in Table 1. It should be noted that the values of the molecular parameters are given in reduced form, with component one always taken as reference. For the sake of simplicity, they

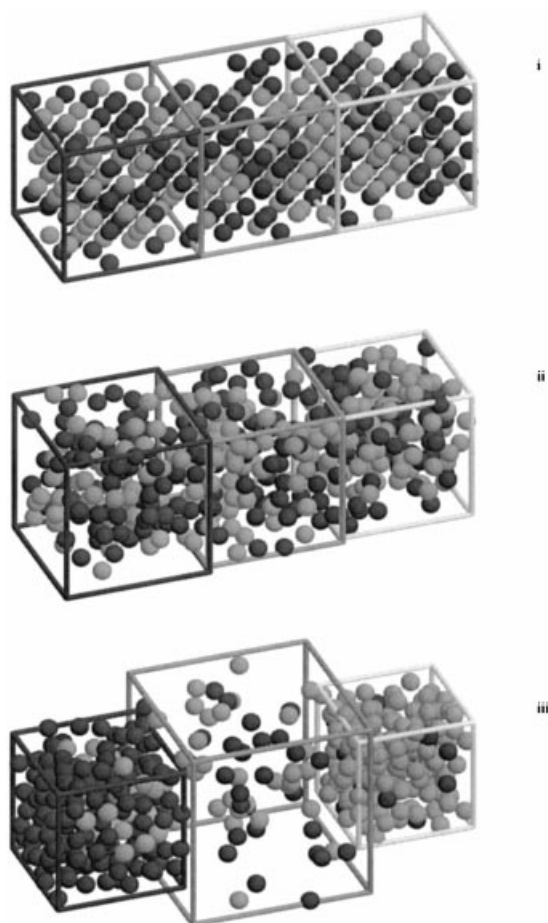


Fig. 4 Evolution of a three-box Gibbs Ensemble Monte Carlo simulation run: (i) in the initial configuration the particles representing the two components of the mixture are placed randomly in a face-centred cubic lattice in three boxes with the same volume, density and composition; (ii) after the first few simulation cycles, the initial configuration ‘melts down’ and the boxes start changing their density and composition; (iii) at last the simulation attains the equilibrium conditions, with each simulation box exhibiting the composition and density characteristic of a given phase.

will be denoted, from now on, by the numerator alone (thus ϵ_{12} stands for $\epsilon_{12}/\epsilon_{12}$). The locations of the first three mixtures (null Z_3 and Z_4) are also included in the global phase diagram of Fig. 2.

TYPE I

Type I mixtures do not exhibit liquid-liquid immiscibility and were the first to be studied by GEMC simulation when the method was extended to mixtures [25]. The two components are miscible, in both phases, over the whole composition range. In the p - T - x space, the phase diagram is represented by two smooth surfaces which merge along three lines—the vapour pressure curves of the two components and the mixture critical line (Fig. 5, I). A simpler representation would be obtained in a p - T - μ diagram (where μ is the chemical potential of the species), since phase equilibrium conditions require that the chemical potential is the same in all phases. The geometric representation is then reduced to a single sweeping surface. A good architectural example of this is the roof that hangs over the vast plaza of the Portuguese Pavilion at EXPO’98, Lisbon (later to become the Government House), designed by Alvaro Siza (Fig. 6, I). Type I mixtures were used to define the reference set of reduced molecular parameters (Table 1) and to check the validity of the extended simulation algorithms (comparing two- and three-box simulation results). Simulations were performed at five different state points (from $T^* = 1.1$ to $T^* = 1.5$ in reduced

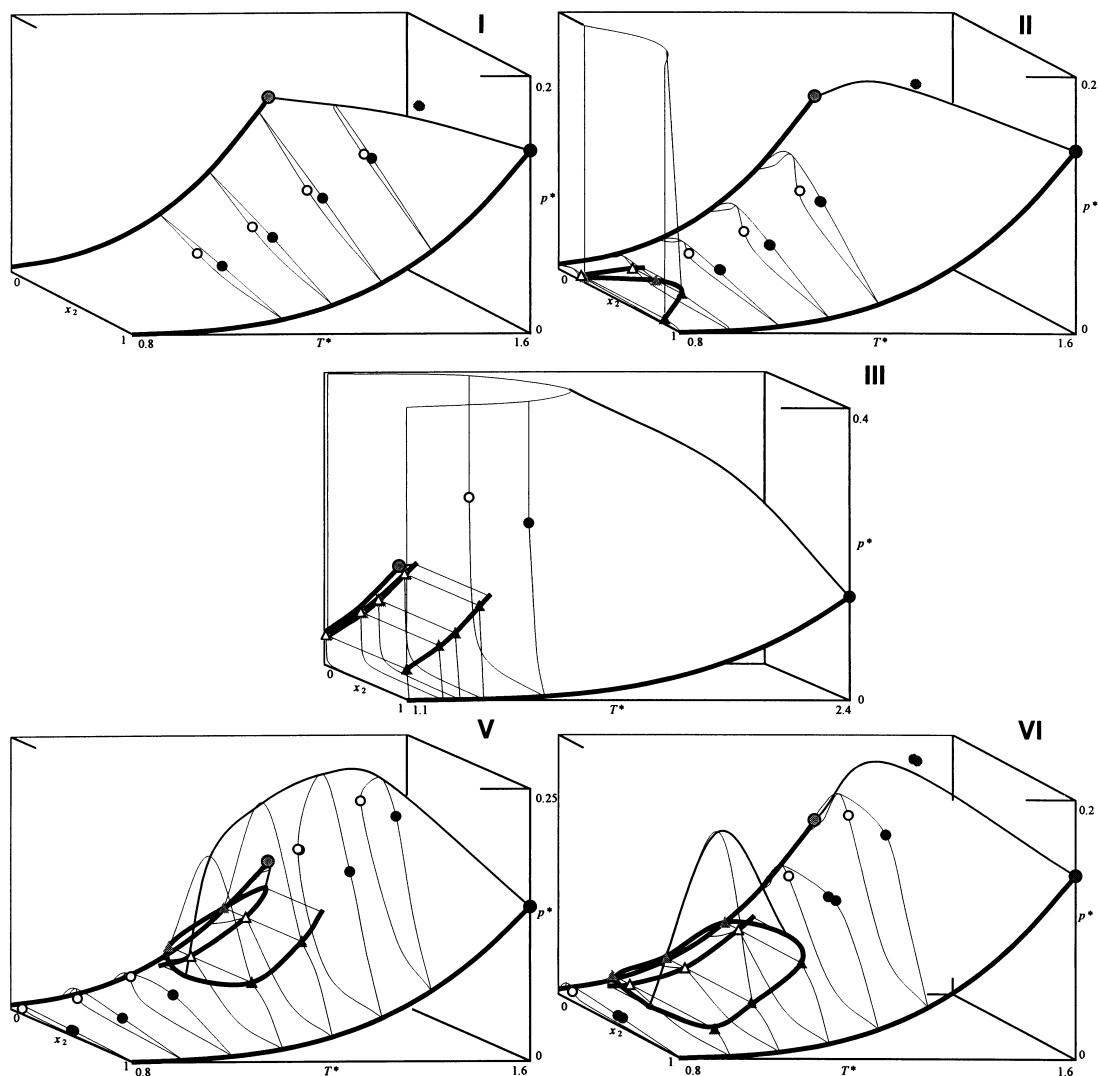


Fig. 5 Fluid phase diagrams (p - T - x representation) of the five binary mixtures studied by simulation. All variables are shown in reduced form. Simulation data [24] are represented as black and white circles (liquid-gas equilibrium), dark circles (single-phase) and black and white triangles (liquid-liquid-gas equilibrium). Thick lines represent the saturation curves of the pure species and the three-phase lines of the mixtures. Medium-thin lines show the loci of the mixtures' critical curves. Very thin lines depict liquid-vapour, liquid-liquid and liquid-liquid-vapour equilibrium lines at the temperature of each simulation run. These lines are drawn only as a visual guide.

Table 1 Molecular interaction parameters (Lennard-Jones (12-6) potential) used during the simulation of five different types of binary mixture

System type	$\epsilon_{22}/\epsilon_{11}$	$\epsilon_{12}/\epsilon_{11}$	σ_{22}/σ_{11}	σ_{12}/σ_{11}	Z_1	Z_2	Z_3	Z_4
I	1.2	1.12	1	1	0.091	-0.018	0	0
II	1.2	0.93	1	1	0.091	0.154	0	0
III	1.8	1.07	1	1	0.286	0.233	0	0
V	1.2	0.76	1	0.82	0.091	0.309	0	0.18
VI	1.2	0.82	1	0.85	0.091	0.254	0	0.15

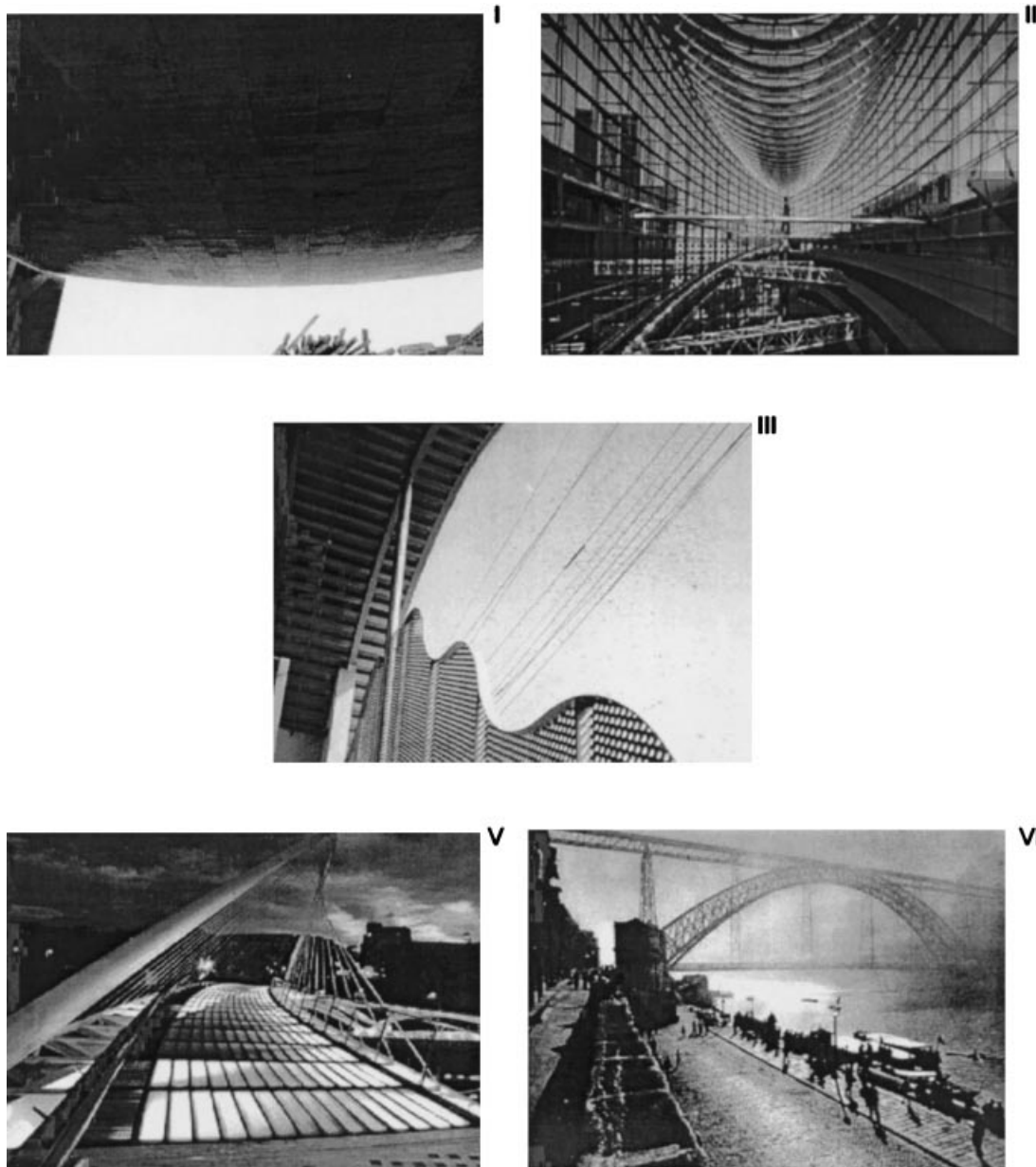


Fig. 6 Architecture through the eyes of a thermodynamicist (cf. Fig. 4 and text). I: Álvaro Siza, Portuguese Pavilion, EXPO'98, Lisbon, Portugal (1998) (photo: José M. Rodrigues); II: Rafael Viñoly, International Forum, Tokyo; Japan (1997); III: Itsuko Hasegawa, Private House, Nerima District, Tokyo, Japan (1986); V: Santiago Calatrava, Campovolantin Footbridge, Bilbao, Spain (1997); VI: Teófilo Seyrig, Dom Luís Bridge, Oporto, Portugal (1886) (photo: Helga Glassner, 1942).

temperature T^* , $T^* = kT/\epsilon_{11}$, for the equimolar global composition, until the mixture's gas-liquid critical curve was reached and crossed.

TYPE II

Type II mixtures had already been simulated by GEMC when the method was extended to more than two simulation boxes/two phases at equilibrium [23]. In the present study, type II behaviour (in fact IIA, cf. Fig. 2) was obtained simply by lowering, by about 17%, the value of the cross interaction parameter ϵ_{12} in the reference set. This leads to liquid-liquid immiscibility at low temperatures and to the formation of an

upper critical solution temperature line terminating at an upper critical end-point, UCEP. In this case, the three-phase line pressure lies above the pressures of both pure components, a fact that implies the presence of a positive azeotrope in the system. The architectural equivalent of azeotropy is fairly common. A recent and striking example is the International Terminal in Waterloo Station, London (1993), designed by Nicholas Grimshaw & Partners (Fig. 7).

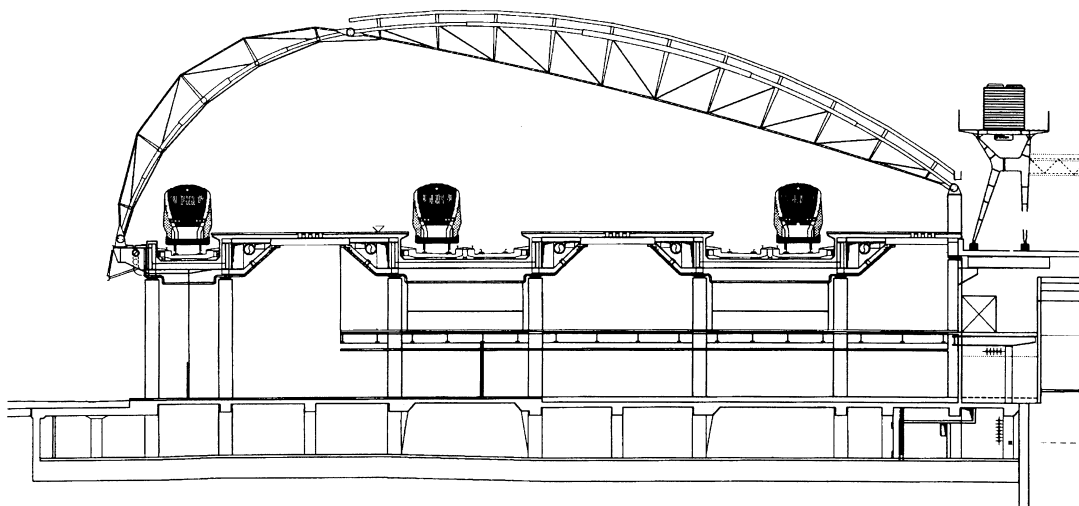


Fig. 7 Cross-section of the International Terminal at Waterloo Station, London. © Nicholas Grimshaw & Partners Ltd (1993).

Simulation runs were performed at six different temperatures, from $T^* = 0.8$ to $T^* = 1.4$, for the equimolar global composition, both below and above the UCEP (Fig. 5, II). An imposing architectural counterpart is the Tokyo International Forum built in 1992–96 to a design by Rafael Vifoly (Fig. 6, II). In the photograph the observer is placed right in the middle of the immiscibility funnel which rises vertically and cuts through the liquid-vapour equilibrium surfaces.

TYPE III

The three-phase liquid-liquid-gas equilibrium phenomenon can vanish either because the two liquids start mixing or because one of them and the gas reach a gas-liquid critical point. Both situations occur at the so called upper critical end-point (UCEP)—the first in a type II mixture, the second a characteristic of type III behaviour. This means that in a type III mixture the gas-liquid critical curve is no longer a continuous line between the two pure component critical points: the critical point of the more volatile component is connected to the UCEP and the gas-‘fluid’ critical line, which starts at the critical point of the less volatile component, takes off to the high-pressure region, eventually reaching the solid-liquid line (cf. Fig. 1, III). This line is often undulating in shape, exhibiting maxima and minima.

Japanese architecture appears fond of such structural elements. An example is the staircase of a private house designed by Itsuko Hasegawa (1986) in the Nerima district, Tokyo (Fig. 6, III). To fully appreciate the architectural analogy, the observer must adopt a yoga position, standing on his/her head, upside-down. . . The edge of the roof above the staircase approximates the vapour pressure curve and meets the critical line mimicked by the wavy handrail (for a better understanding of the analogy, the reader should turn the illustration upside-down).

To generate type III behaviour, the volatility difference between the two components had to be increased, while the relative strength of the cross interaction ϵ_{12} had to decrease. This was achieved by augmenting the energy parameter of the less volatile component to $\epsilon_{22} = 1.8$ and diminishing the value of ϵ_{12} to $\epsilon_{12} = 1.07$. (Z_1 increases from 0.091 to 0.286 and, likewise, Z_2 goes up from -0.018 to 0.233) Simulations at five different temperatures (values of T^* between 1.1 and 1.5) and equimolar global composition, before and after the UCEP, are shown in the phase diagram presented in Fig. 5, III.

TYPES IV AND V

Type IV to type VI mixtures exhibit both lower and upper critical end-points, LCEP and UCEP. Type IV will not be discussed here because, from the conceptual point of view, it represents a ‘hybrid’ of types II and V (cf. Fig. 1).

A lower critical end-point (demixing of two liquids as the temperature is raised) is harder to explain than its upper analogue, but can be viewed as the result of two opposing driving forces: strong cross interactions between the two components and a large volatility difference between them. At low temperatures/pressures the more intense cross-interactions will determine the equilibrium conditions and the system will not exhibit liquid-liquid immiscibility (the volatility difference is irrelevant at low pressures). As the temperature/pressure is raised, the balance is upset and demixing will occur as a result of a sufficiently large volatility difference between the two components. This scenario corresponds to a typical type V mixture, found for large values of Z_1 , negative values of Z_2 and zero values of Z_3 and Z_4 (cf. Fig. 2). However, these are not the only circumstances under which a LCEP can emerge; they are, in fact, rather restrictive conditions since the large difference in volatility between the components leads, in most cases, to relatively short three-phase lines in type V mixtures and prevent (or limit) the existence of type VI behaviour. What happens is that the UCEP breaks the continuity of the gas-liquid critical curve between the critical points of the pure components.

In this work, an alternative way of finding a type V mixture has been devised. (Versatility is the name of the game whenever phase diagrams are directly simulated from molecular potential ratios.) One of the two opposing forces responsible for the LCEP is no longer the big volatility difference between components (Z_1), but rather the small value of the cross interaction diameter (Z_4). At low temperature/high density the system will form a single liquid phase because the molecules of the two components ‘fit’ together in a non-random, close-packed mixture. As temperature is raised and density decreases, this situation is lost and the weak cross-interactions lead to demixing. The set of parameters used for the simulation illustrates this strategy: the volatility difference between components is set at the (low) reference value, $\epsilon_{22} = 1.2$ ($Z_1 = 0.091$), ϵ_{12} is set at $\epsilon_{12} = 0.76$ (reflecting weak cross-interactions, i.e. large $Z_2 = 0.309$) and the cross interaction diameter is set at a value of $\sigma_{12} = 0.82$ (down from the reference value of $\sigma_{12} = 1$). Seven runs were performed between $T^* = 0.8$ and $T^* = 1.4$ for the equimolar global composition. Figure 5, V depicts simulation points situated below the LCEP, above the UCEP and between the two.

The analogue should be a work of art that stands and lives by the balance between two opposing forces: the tension of steel pitted against the pull of gravity—in other words, a suspension bridge. A stunning example is Santiago Calatrava’s Campovolantin footbridge in Bilbao (1997). As in a type V mixture, the balance (and beauty) is achieved by the exquisite interaction between two curves: the suspension arch and the bent bridge platform (cf. Figs 5, V and 6, V).

TYPE VI MIXTURE

At this point, the choice of a set of parameters that leads to a type VI behaviour (from a type V one), should be quite straightforward. If the cross-interactions are made less unfavourable, the locus of the UCEP moves to lower temperatures/pressures, fails to interact with the gas-liquid critical line and forms the liquid-liquid immiscibility closed loop. The gas-liquid critical line then resumes its continuity between the critical points of the two pure components.

Accordingly, ϵ_{12} was raised from a value of 0.76 to 0.82 (stronger cross-interactions, smaller Z_2). The cross-interaction diameter σ_{12} was also increased from 0.82 to 0.85, so that the LCEP could be observed at lower temperatures and the three-phase line did not become too short. Six simulation runs were performed between $T^* = 0.8$ and $T^* = 1.4$ for the equimolar global composition. The points obtained are situated below the LCEP, above the UCEP, between the two and above the gas-liquid critical line (Fig. 5, VI).

For the last architectural/engineering example we go back to the dawn of the studies of phase diagrams and select the Dom Luís Bridge, in Oporto, Portugal (the city that plays host to the 15th International Conference on Chemical Thermodynamics). A comparison between Fig. 5, VI and 6, VI shows that the

arch corresponds to the locus of critical solution temperatures whereas the lower crossing road, uniting the two banks of the river Douro, stands for the three-phase line. Built by Teófilo Seyrig in 1886, the Dom Luís Bridge is also the earliest of the five works of art evoked in this paper. It is a fitting choice because, at that time, van der Waals was deeply involved in the formulation of his theory of mixtures. At the end of the 19th century, Portuguese engineers and workers were also doing thermodynamics by other means.

ACKNOWLEDGEMENTS

One of us (J.C.G.C.) would like to thank Prof. Roald Hoffmann for the hospitality and stimulating discussions during his stay at Cornell University (Spring Semester, 1998). In matters pertaining to liquids and liquid mixtures, both of us have been inspired by the teachings of Prof. John Rowlinson and also by his devotion to the memory and works of van der Waals.

REFERENCES

- 1 *Encyclopædia Britannica*. William Benton, Chicago (1969).
- 2 Carolus Linnæus. *Species plantarum* (1753); *Genera Plantarum*, 5th edn (1754).
- 3 L. Howard. *Phil. Mag.* **16**, 97 (1803).
- 4 J. D. van der Waals. *Over de Continuïteit van den Gas- en Vloeïstoofstand*. Thesis. Leiden (1873).
- 5 J. D. van der Waals. *Arch. Néerl.* **24**, 1 (1891).
- 6 H. A. Lorentz. *Ann. Physik* **12**(127), 660 (1881).
- 7 J. D. van der Waals. *Die Continuität des Gasförmigen und Flüssigen Zustandes, 2. Teil., Binäre Gemische*. Barth, Leipzig (1900).
- 8 J. P. Kuenen. *Commun. Phys. Lab. Univ. Leiden*, No. 4 (1892).
- 9 J. D. van der Waals. *Proc. Sec. Sci. Kon. Akad. Wet. Amsterdam* **15**, 602 (1913).
- 10 H. Kammerling Onnes. *Commun. Phys. Lab., Univ. Leiden*, Nos 119, 120, 122 (1911).
- 11 B. H. Sage, W. N. Lacey. *Volumetric and Phase Behavior of Hydrocarbons*. Stanford University Press, Palo Alto, CA (1939).
- 12 I. R. Krichevskii. *Technique of Physicochemical Investigations at High and Superhigh Pressures*, 3rd edn. Izd. Khimliya, Moscow (1965).
- 13 G. M. Schneider. In *Chemical Thermodynamics, Specialist Periodical Reports* (M. L. McGlashan, ed.), Vol. 2, pp. 71. Chemical Society, London (1978).
- 14 J. C. G. Calado. *Rev. Port. Quim.* **1** (III series), 31 (1994).
- 15 J. O. Hirschfelder, C. F. Curtiss, R. Byron Bird. *Molecular Theory of Gases and Liquids*. John Wiley, New York (1954).
- 16 B. J. Alder, T. E. Wainwright. *J. Chem. Phys.* **33**, 1439 (1960).
- 17 P. H. van Konynenburg, R. L. Scott. *Phil. Trans.* **A298**, 495 (1980).
- 18 L. Z. Boshkov. *Doklady Akademii Nauk SSSR* **294**, 901 (1987).
- 19 L. V. Yelash, T. Kraska. *Ber. Bunsenges. Phys. Chem.* **102**, 213 (1998).
- 20 A. Bolz, U. K. Deiters, C. J. Peters, T. W. de Loos. *Pure Appl. Chem.* **70** (11), 2233 (1998).
- 21 H. Hartl, F. Mahdjour-Hassan-Abadi. *Angew. Chem. Int. Ed. Engl.* **33**, 1841 (1994).
- 22 A. Z. Panagiotopoulos. *Molec. Phys.* **61**, 813 (1987).
- 23 J. N. Canongia Lopes, D. J. Tildesley. *Molec. Phys.* **92**, 187 (1997).
- 24 J. N. Canongia Lopes. *Molec. Phys.* **96**, 1649 (1999).
- 25 A. Z. Panagiotopoulos, N. Quirke, M. Stapleton, D. J. Tildesley. *Molec. Phys.* **63**, 527 (1988).